

SoilMoistureMapper: a GNSS-R approach for soil moisture retrieval on UAV

Volkan Senyurek^{1*}, Mehedi Farhad², Ali C. Gurbuz², Mehmet Kurum², Robert Moorhead¹

Geosystems Research Institute, Mississippi State University¹
Dept. of Electrical and Computer Eng. Mississippi State University²
Starkville, MS, USA
volkan@gri.msstate.edu

Abstract

Measuring of distribution of the soil moisture (SM) content is an essential requirement in precision agriculture. This paper demonstrates practical and low-cost soil moisture mapping techniques based on Global Navigation Satellite System (GNSS) Reflectometry (GNSS-R) observations via a small-size unmanned-aerial vehicle (UAV). An SM estimation model is developed using a random forest (RF) machine-learning (ML) algorithm combining GNSS-R signals with ancillary vegetation indices from a multispectral camera. The ML model is trained and tested using in-situ data from eight SM probes located in a 2.48ha farm. The study results showed that SM maps of the field can be obtained with about 13 mins flight with $5\text{m} \times 5\text{m}$ spatial resolution. The developed ML model reached RMSE of $0.032\text{m}^3\text{m}^{-3}$ and R-value of 0.93 in 10-fold cross-validation.

The traditional way of measuring SM content is to use in-situ SM probes. Although this technique is accurate and reliable, it can be costly and inefficient for precision agriculture. Over the last decades, with the progress of remote sensing techniques, microwave-based satellite missions have been launched for regional and global SM measurements. Soil Moisture Active Passive (SMAP) (Entekhabi et al. 2010) and The European Space Agency's (ESA) Soil Moisture and Ocean Salinity (SMOS) (Kerr et al. 2016) are two well known dedicated spaceborne missions that use L-band radiometer to measure surface SM. Both missions provide 36-km spatial and 1-3 days temporal resolution on a global scale. Sentinel-1 is another spaceborne mission that uses C-band synthetic aperture radar and provides 1-km spatial and 6-12 days temporal resolution (Paloscia et al. 2013). Global navigation satellite system reflectometry (GNSS-R) is a signal-of-opportunity (SoOP) application based on bistatic radar configuration. In GNSS-R, all navigation satellites work as transmitters, and passive receivers collect reflected signals from the earth's surface. NASA's Cyclone GNSS-R (CYGNSS) mission contains eight low orbit satellites that collected reflected GNSS signals from on the ground. Although this mission was designed to improve hurricane forecasting, many studies showed that its land observation could

be used in SM estimation (Chew and Small 2018; Al-Khaldi et al. 2019; Eroglu et al. 2019; Senyurek et al. 2020; Yan et al. 2020). With the help of the low apogee altitude(536 Km) of the CYGNSS constellation, it provides higher spatial ($7\text{Km} \times 0.5\text{Km}$ for coherent scattering) and temporal resolution (0.5 and 0.1 visits/day for $9\text{-km} \times 9\text{-km}$ aggregated grids) than other spaceborne SM missions. With the help of the low apogee altitude(536 Km) of the CYGNSS constellation, it provides higher spatial ($7\text{Km} \times 0.5\text{Km}$ for coherent scattering) and temporal resolution (0.5 - 0.1 visits/day for $9\text{-km} \times 9\text{-km}$ aggregated grids) than other spaceborne SM missions. However, still, its spatiotemporal resolution is not enough for site-specific PA applications. This study demonstrated that GNSS-R-based SM estimation could be achieved using a small drone and a low-cost GNSS receiver in a high resolution. We developed an ML SM retrieval model that uses surface reflected signals and vegetation indexes as input. The model was trained and validated with *in-situ* measurements.

SoilMoistureMapper structure

Fig. 1 shows the concept and the steps of the UAV-based SM retrieval structure. A UAV equipped with a GNSS receiver follows a predefined flight plan for each experiment. During the flight, the GNSS receiver collects all available reflected signals from the field surface simultaneously. A multispectral camera provides spectral images (blue, green, red, red edge, and near-IR bands) to calculate related vegetation indices used as ancillary data in the developed SM model. Eight SM probes are placed at different locations in the field as ground truth SM data sources for ML model training and validation.

Hardware and study field

A U-blox GNSS receiver with its onboard mini-computer and A multispectral camera (redEdge-MX) is attached underneath of UAV (550m carbon fiber frame with PixHawk flight controlled) Fig. 2.

Forty flight experiments were performed between June 2020 and October 2020 on a 2.48ha farm at The R. R. Foil Plant Science Research Center, Mississippi State University, Starkville, MS, the USA. The flight parameters are set as 15-meter flight altitude, 5m/s flight speed, and 13 min flight

*This research was funded by USDA Agricultural Research Service(USDA-ARS), Award NACA 58-6064-9-007
Copyright © 2022, Association for the Advancement of Artificial Intelligence (www.aaai.org). All rights reserved.

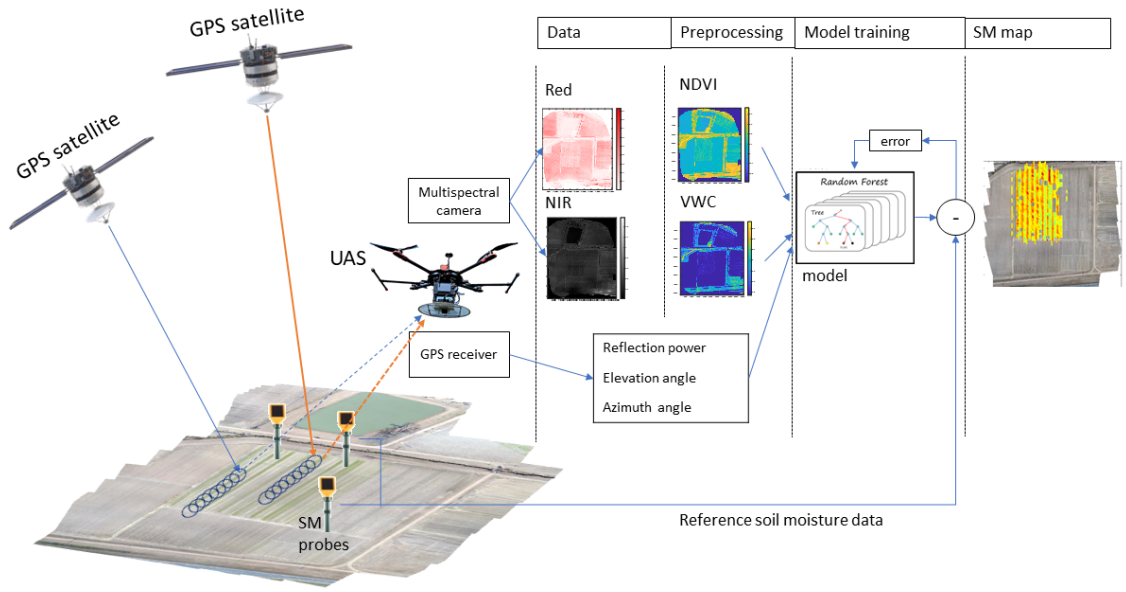


Figure 1: Simplified structure of UAV based SM retrieval.

time for all experiments. Fig. 3 shows the study field and predefined flight path.



Figure 2: The UAV equipped with u-blox GPS receiver and multispectral camera

Data preparation and ML model development

Specular reflection points are calculated using NASA's GPS orbit data product and the current location of UAV for each reflected GPS signal. Then for each specular point, carrier-to-noise density (C/N_0), elevation, and azimuth angles are extracted from recorded National Marine Electronics Association (NMEA) messages.

The previous studies showed that L-band microwaves are not only sensitive to SM also vegetation occupancy. Vegetation cover attenuates and reflects the incident signals (Guo



Figure 3: Study field and the flight path.

et al. 2013). An ML model for SM retrieval should consider vegetation effects in the model development process. In this study, we calculate Normalized difference vegetation index (NDVI) and vegetation water content (VWC) indexes from red and near-IR spectral bands images using equations in (Chan et al. 2013).

The spatial resolution of the study is $5\text{m} \times 5\text{m}$ because of the 5m/s flight speed and 1 Hz GPS sampling rate. So all five input features (C/N0, elevation angle, azimuth angle, NDVI and VWC) are gridded into $5\text{m} \times 5\text{m}$ grids.

An RF regression algorithm with ten trees and a maximum split size of 6 for each tree is utilized as an ML algorithm. The RF model is trained using a least-squares boosting ensemble strategy with a learning rate of 0.75. The RF model is trained and validated with input features (C/N0, elevation angle, azimuth, NDVI, and VWC) and soil moisture measurements from SM *in-situ* probes in 10-fold and leave-one-probe cross-validation fashion. The performance of the developed SM model is evaluated by calculating RMSE, unbiased RMSE (ubRMSE), and R-value metrics.

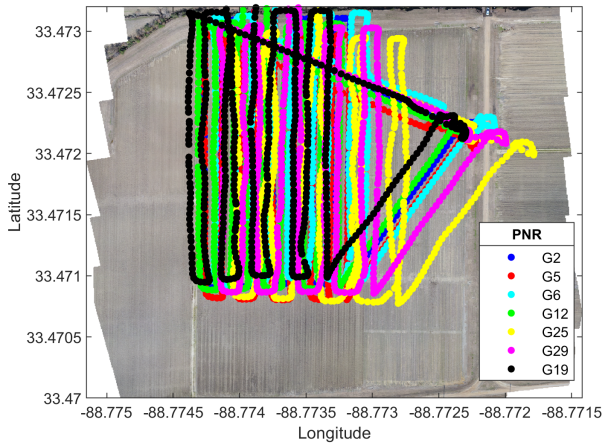


Figure 4: Distribution of calculated specular point in the study filed on 10 July 2020.

Results and Discussions

A total of 50 flights were performed between 7 January 2020 and 15 October 2020. The GNSS receiver recorded signals from an average of $10.14 (\pm 1.35)$ GPS satellites during the flights. During the whole experiment, a total of 209757 observations were recorded. The observations that correspond to elevation angles lower than 15 degrees and C/N0 smaller than 15 dB were removed from the dataset. After the data filtering process, the average number of usable GPS satellites and the average number of specular points decreased to $7.56 (\pm 0.8)$ and $4736 (\pm 878)$ per flight. We calculated the average coverage rate of the field as 88% in a single flight. We also observed that the area rate with multiple specular point observation is 82%. The coverage rates and multiple sampled rates were calculated based on $5\text{m} \times 5\text{m}$ grid cells. Table 1 summarizes all the statistics about experiments, and

Fig. 4 shows the distribution of specular points on 10 July 2020. The figure shows there are pretty much multiple observations for many grids. If a grid has multiple observations, multiple SM estimations are averaged and assigned as the SM estimations of the grid.

Fig. 5(a-d) shows the images of C/N0, elevation angle, NDVI, and estimated soil moisture maps on 10 July 2020. Although the proposed UAV-based method provides estimations for most of the study area, there are still some gaps without SM estimation since fewer GPS satellites or the quality of observations. The results show that a 13 min flight covers most of the parts of a 2.48ha field. Fig. 5 shows there are pretty much multiple observations for many grids. If a grid has multiple observations, multiple SM estimations are averaged and assigned as the SM estimations of the grid. Fig. 5(d) shows SM differences between the upper (corn) and lower (cotton) parts of the field. In addition, the relatively dry SM of the alley between the crops field can be seen from the map.

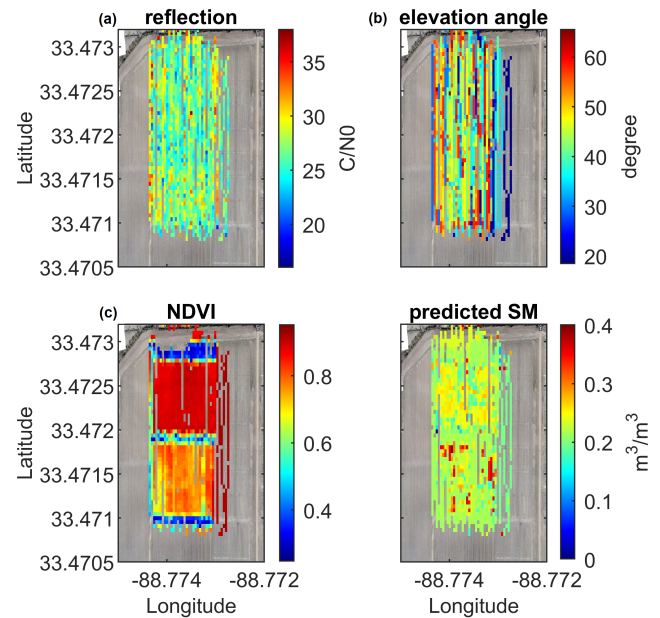


Figure 5: Measured inputs and estimated SM on 10 July 2020. (a-b) reflection power and elevation angle from GNSS receiver, (c) NDVI, (d) SM.

The performance validation of the proposed UAV-based SM model was performed against eight *in-situ* SM probes measurements. The performance metrics, RMSE, ubRMSE, and R-value, were calculated in 10-fold and leave-one-probe-out cross-validation fashions. Table 2 summarizes the overall performance of the proposed model. The ML model reached the overall RMSE of $0.032\text{ m}^3\text{m}^{-3}$ and overall R-value of 0.93 in 10-fold cross-validation. These scores were obtained as $0.068\text{ m}^3\text{m}^{-3}$ and 0.40 in leave-one-probe-out cross-validation. Fig. 6 provides a temporal comparison of UAS-based SM estimates against SM probe measurements for four SM probes. The figure shows that UAS-

# of flights	Avg. seen GPSs	Avg. usable GPSs	Avg. sampled specular points	Avg. coverage rate	Avg. multiple SP rate
40	10.64 (± 1.48)	7.65 (± 0.8)	5378 (± 629)	0.86 (± 0.07)	0.82 (± 0.1)

Table 1: Flights and data statistics.

based GNSS-R SM estimates follow the in-situ measurements closely. However, slightly lower leave-one-probe-out cross-validation performance indicates that to obtain a better site-independent model, more in-situ measurements from different field locations should be added.

Cross-validation	RMSE (m^3m^{-3})	R-value
10-fold	0.032	0.93
leave-one-probe-out	0.068	0.40

Table 2: Overall performance metrics for different cross-validation methods

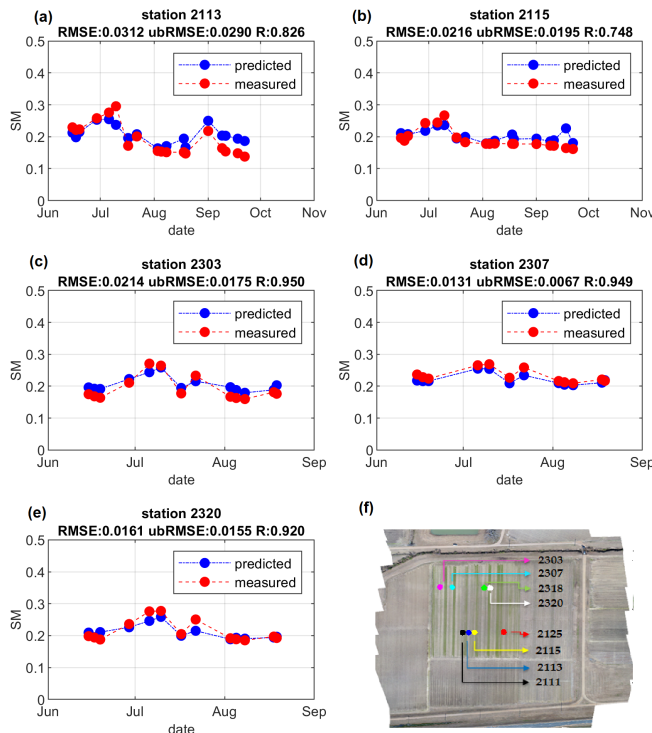


Figure 6: (a-e) time series of measured and estimated SMC in 10-fold cross-validation for selected SM probes, (f) location of SM probes.

Conclusion

This study demonstrated that a simple GNSS receiver could collect reflected GNSS signals from the agricultural field. In combination with vegetation indices via a multispectral camera, reflected GNSS signals can estimate SM value with a high resolution. The obtained performance score of the model using different cross-validation techniques shows the capability of the application. Compared to the traditional soil

moisture estimations based on a few soil moisture samples averaged across the farm, The proposed method enables accurate prediction in the agricultural application to identify dry/wet spots and water-stressed crops. As a future study, different flight plans (flight altitude, flight speed, and flight duration) will be tested for more accurate and better spatial resolution. Instead of a multispectral camera, a 3D Lidar may provide more detailed vegetation information that can help improve ML model performance.

References

- Al-Khaldi, M.; Johnson, J.; O'Brien, A.; Balenzano, A.; et al. 2019. Time-Series Retrieval of Soil Moisture Using CYGNSS. *IEEE Transactions on Geoscience and Remote Sensing*, 57(7): 4322–4331.
- Chan, S.; Bindlish, R.; Hunt, R.; Jackson, T.; and Kimball, J. 2013. Vegetation Water Content. *Jet Propulsion Laboratory, California Institute of Technology: Pasadena, CA, USA*.
- Chew, C. C.; and Small, E. E. 2018. Soil Moisture Sensing Using Spaceborne GNSS Reflections: Comparison of CYGNSS Reflectivity to SMAP Soil Moisture. *Geophys. Res. Lett.*, 45(9): 4049–4057.
- Entekhabi, D.; Njoku, E. G.; O'Neill, P. E.; Kellogg, K. H.; Crow, W. T.; Edelstein, W. N.; Entin, J. K.; Goodman, S. D.; Jackson, T. J.; Johnson, J.; et al. 2010. The soil moisture active passive (SMAP) mission. *Proceedings of the IEEE*, 98(5): 704–716.
- Eroglu, O.; Kurum, M.; Boyd, D.; and Gurbuz, A. C. 2019. High Spatio-Temporal Resolution CYGNSS Soil Moisture Estimates Using Artificial Neural Networks. *Remote Sens.*, 11(19): 2272.
- Guo, P.; Shi, J.; Liu, Q.; and Du, J. 2013. A new algorithm for soil moisture retrieval with L-band radiometer. *IEEE Journal of selected topics in applied earth observations and remote sensing*, 6(3): 1147–1155.
- Kerr, Y. H.; Al-Yaari, A.; Rodriguez-Fernandez, N.; Parrons, M.; Molero, B.; Leroux, D.; Bircher, S.; Mahmoodi, A.; Mialon, A.; Richaume, P.; et al. 2016. Overview of SMOS performance in terms of global soil moisture monitoring after six years in operation. *Remote Sensing of Environment*, 180: 40–63.
- Paloscia, S.; Pettinato, S.; Santi, E.; Notarnicola, C.; Pasolli, L.; and Reppucci, A. 2013. Soil moisture mapping using Sentinel-1 images: Algorithm and preliminary validation. *Remote Sensing of Environment*, 134: 234–248.
- Senyurek, V.; Lei, F.; Boyd, D.; Kurum, M.; Gurbuz, A.; and Moorhead, R. 2020. Machine Learning-Based CYGNSS Soil Moisture Estimates over ISMN sites in CONUS. *Remote Sensing*, 12(7): 1168.
- Yan, Q.; Huang, W.; Jin, S.; and Jia, Y. 2020. Pan-tropical soil moisture mapping based on a three-layer model from CYGNSS GNSS-R data. *Remote Sensing of Environment*, 247: 111944.